JETP Letters, Vol. 73, No. 4, 2001, pp. 192–196. Translated from Pis'ma v Zhurnal Éksperimental'noĭ i Teoreticheskoĭ Fiziki, Vol. 73, No. 4, 2001, pp. 214–219.

Observation of Laser-Induced Local Modification of Magnetic Order in Transition Metal Layers

A. M. Alekseev[1], Yu. K. Verevkin[2], N. V. Vostokov[3], V. N. Petryakov[2], N. I. Polushkin[3,4], A. F. Popkov[1], and N. N. Salashchenko[3]

[1] *Lukin Scientific Research Institute of Physical Problems, Moscow, 103460 Russia*
[2] *Institute of Applied Physics, Russian Academy of Sciences, ul. Ul'yanova 46, Nizhni Novgorod, 603600 Russia*
[3] *Institute of Macrostructure Physics, Russian Academy of Sciences, Nizhni Novgorod, 603600 Russia*
[4] *e-mail: nip@ipm.sci-nnov.ru*

Received January 15, 2001

Laser-induced local modifications of magnetic order in thin Fe–Cr layers were investigated. Local modification in the layers were induced by interfering laser beams. The results of the study give evidence for the formation of submicron-sized anisotropically shaped ferromagnetic regions with a well-defined direction of the easy magnetic axis in the interference maxima at the modification threshold. It was also found that the magnetic anisotropy of a medium is drastically reduced with changing the shapes of these local regions and distances between them. This may be due to the strengthening of the interaction between the regions through the paramagnetic matrix. © *2001 MAIK "Nauka/Interperiodica".*

PACS numbers: 75.70.Kw; 75.60.Jk; 75.50.Bb; 75.50.Cc

It is known [1–3] that the Fe(Co)-based nanocomposite alloys of 3*d* metals may not possess long-range magnetic order at the concentrations of magnetic component as high as 70–75 at. %. In [1], a model was suggested according to which such alloys are composed of superparamagnetic clusters in a nonmagnetic medium. As the concentration of magnetic atoms increases, the cluster formation becomes more intense and, eventually, a concentration is achieved (percolation threshold) at which the long-range magnetic order is extended over the whole material.

Another way of creating a magnetically ordered state in alloys (without changing the mean concentration of the magnetic component) consists in heating a metallic medium by an intense (~1 J/cm^2) short (~10 ns) laser pulse to a temperature higher than the melting point, to initiate diffusional mixing of the alloy components, and its fast cooling (with a rate of ~10^{10} K/s) after the pulse. This gives rise to a metastable supersaturated solid solution whose magnetic properties are sensitive to the positional and chemical short-range orders in the system [4]. In [5, 6], we reported the observation of thermo- and laser-induced modifications of the magnetic order in thin-film (< 100 nm) mixtures of the Fe–C, Co–C, and Fe–Cr types. The major experimental fact was that after the laser pulse with an energy density of 200–400 mJ/cm^2, the originally (super)paramagnetic medium became ferromagnetic at room temperature in a certain (rather narrow) concentration range of the magnetic component, with the saturation magnetization of the resulting ferromagnet being close to the value in the bulk Fe and Co samples.

In this work, laser-induced magnetic ordering was used to produce a regular grating of small ferromagnetic elements. The sizes of these elements are limited in all three directions and comparable with the key micromagnetic parameters: exchange length (10 nm) and domain wall thickness (10–100 nm). As regards the physics of magnetization reversal, these elements are intermediate between the multidomain and single-domain systems. The physical behavior of this system is noteworthy in two aspects. First, it is important to determine the conditions for the formation of single-domain (ferro)magnetic regions in the course of local modification of a paramagnetic medium. Second, it is of interest to study the specific features of magnetization reversal for a system of magnetically hard particles in a magnetically soft medium. Interest in the structures of small magnetic objects has arisen because such systems are viewed as an alternative material for the design of new magnetic ultrahigh-density recording and data storage devices [7, 8].

In this work, local modification was accomplished by the coherent UV laser beams that are capable of creating an interference grating with submicron spacing (down to 200 nm) at the sample surface. The sizes of modified magnetic elements can preliminary be estimated from the thermal diffusion length $\sqrt{a\tau}$, where a is the thermal conductivity coefficient and τ is the heat pulse duration. For a pulse duration of no more than several nanoseconds and a pulse energy close to the magnetic transformation threshold, the sizes of the elements can be expected not to exceed 100 nm.

0021-3640/01/7304-0192$21.00

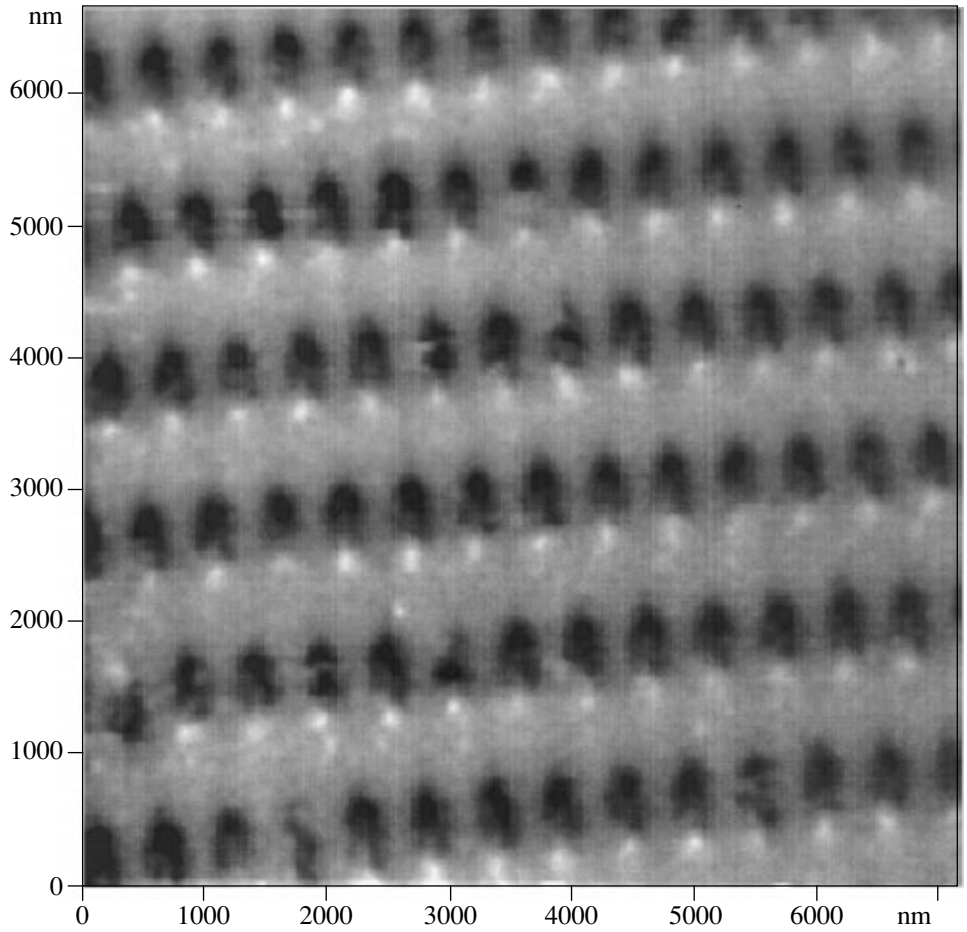

Fig. 1. The MFM image of the surface of a $Fe_{0.7}Cr_{0.3}$ layer irradiated by two pairs of beams with energy density $E = 250$ mJ/cm^2. The asymmetrically shaped dipoles are clearly seen. The image is obtained for a residual state after the magnetization along the dipole direction.

The starting alloys for the subsequent laser annealing were thin layers (15–20 nm) prepared by the alternate deposition of small portions (0.3–0.5 nm) of Fe(Co) and Cr(C) on silicon substrates, with the Nd^{3+} laser radiation being focused onto the targets placed in a vacuum chamber. The absence of ferromagnetic order in the starting samples and its appearance after irradiation was monitored by the spectra of ferromagnetic resonance. These data were used to determine the optimum concentration of the magnetic component in a mixture for which the starting sample did not yet show a magnetic response at room temperature while, after irradiation, a well-defined signal of ferromagnetic resonance appeared.

The magnetic structures were produced using a narrow-band (0.04 cm^{-1}) XeCl eximer laser ($\lambda = 308$ nm) with a pulse energy up to 50 mJ and a pulse duration of 8 ns. Laser emission was monochromatized by the intracavity mode selection using a Fabry–Pérot interferometer to provide a contrast interference pattern throughout the whole cross section of the laser beam. To produce a two-dimensional grating of modified local regions, the laser radiation was split into two pairs of beams that were incident on the sample at different angles in two mutually perpendicular planes. The intensity distribution in the interference maxima was extended along the axis in the plane of the smaller angle of incidence, with the aspect ratio corresponding to the ratio of angles of incidence. The total area of the array was determined from the diffraction of a HeNe laser radiation by the grating. Depending on the pulse energy, this area was 5–10 mm^2.

The properties of the gratings were studied by atomic-force (AFM) and magnetic-force (MFM) microscopy, and the magnetic hysteresis loops were measured in the presence of the longitudinal magneto-optical Kerr effect. The AFM/MFM data were recorded on a Solver P47 (NT-MDT, Moscow) scanning probe microscope. Silicon cantilevers sputtered with a ≈30-nm thick Co layer were used as magnetic probes. Resonance frequencies of the probes were equal to 55–120 kHz. Before measurements, the magnetic probe was magnetized along the tip axis while the samples themselves were preliminary magnetized in fields

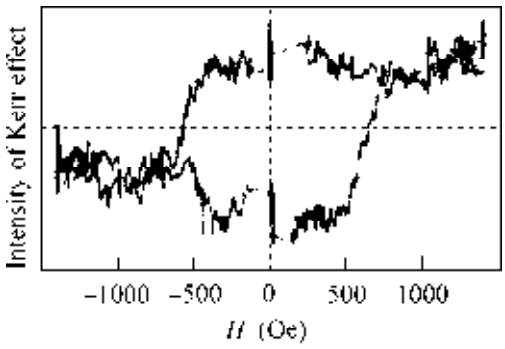

Fig. 2. Magnetization reversal curve for the magnetic elements in a $Fe_{0.7}Cr_{0.3}$ layer subjected to the interference laser annealing (E = 250 mJ/cm^2). The external magnetic field H is applied in the dipole direction.

of up to 1500 Oe aligned in the sample plane with the minor or major axis of the created elements. The distribution of the magnetic force gradient was determined from the phase shift induced in the cantilever oscillations by either attractive or repulsive forces acting on the magnetic tip.

Figure 1 is the MFM image of the surface of a $Fe_{0.7}Cr_{0.3}$ layer after interference irradiation at angles of incidence of 10° and 40° by a laser pulse with an energy density of E = 250 mJ/cm^2. This energy is close to the very threshold of magnetic modification (220–240 mJ/cm^2). It has not yet produced any changes in the surface relief. Nevertheless, a periodic structure of identically oriented asymmetrically shaped dipoles is clearly seen in the MFM image: dark (large) and light (smaller) spots indicate the poles of the magnetic elements. The observed orientation of the dipoles corresponds to the sample premagnetization direction. One can see from the pole positions that the aspect ratio of the ferromagnetic elements equals approximately 1 : 4, in quantitative agreement with the ratio of angles of incidence.

Figure 2 shows the magnetization reversal curve for the same Fe–Cr sample. In this experiment, an external magnetic field was aligned with the dipole orientations in Fig. 1. One can see that this curve has a hysteretic character typical of ferromagnets, and the shape of the hysteresis loop is close to rectangular with a magnetization reversal field of ≈500 Oe. An attempt at reversing magnetization of this sample in the direction perpendicular to the dipole orientation in fields up to 2000 Oe did not affect the magneto-optical response to within the noise level. Therefore, the irradiation of the layer near the magnetic transformation threshold gives rise to a magnetic structure with a well-defined easy magnetization direction corresponding to the orientation of dipoles in the MFM image.

A characteristic feature of the magnetic elements is that their thickness (15–20 nm) is much smaller than their lateral sizes (100 × 400 nm). We carried out micromagnetic modeling of magnetization distribution in the elements with thicknesses 10–20 nm. It follows from the numerical experiments that the magnetic elements show a single-domain behavior at thicknesses less than 12 nm in the case of weak anisotropy or at 15 nm in the case of a uniaxial anisotropy of ~10^6 erg/cm^3. Otherwise, skew-symmetric magnetization distributions with edge spin fixation or a more complex spin configuration with one or two vortices inside the elements are formed. Hence, the magnetic-pole asymmetry observed in our experiments (Fig. 1) may point to the inhomogeneous magnetization distribution in the magnetic elements.

It is of interest to examine the properties of a layer modified with higher-energy laser pulses. Figure 3 is the AFM image of the topography of a surface Fe–Cr layer irradiated by E = 300 mJ/cm^2. This image provides evidence for the formation of craters in the interference maxima as a result of melting and expelling melt toward the periphery of the interference maxima by vapor pressure. The craters are shaped like ellipses with an axes ratio of 1 : 2, and their depth from the bottom to the top of their rims is as large as 8–10 nm. The modification of surface topography is also accompanied by profound changes in the properties of the created magnetic structures. The magnetic hysteresis loops of the same (E = 300 mJ/cm^2) Fe–Cr sample suggest that magnetic anisotropy in the new matrix is strongly reduced (Fig. 4). It is seen that the remanent magnetization of this sample remains close to the saturation magnetization in an external magnetic field oriented along both the major (Y) and the minor (X) crater axes. Nevertheless, it is worth noting that the magnetization reversal loop becomes more rectangular for remagnetization along the X axis (minor axis of the craters in Fig. 3), possibly because of the appearance of the easy magnetic axis in this direction, whereas the magnetization in a "hard" Y direction shows a relatively smooth saturation. The shape of the hysteresis loop in this direction is typical of a strongly dispersive medium [9]. Note that if the system of magnetic elements is well-defined in the topographical images, then the anomalous orientation of the easy magnetic axis occurs even for loose packing of elliptic craters. As the laser energy further increases (350–400 mJ/cm^2), the minor axis of the ellipses increases up to a contact of two neighboring crater rims. However, these relief modifications no longer alter the magnetic behavior of the irradiated samples.

The studies of the morphology and magnetic properties of the Fe–Cr-type systems suggest [2, 3] that they consist of Fe-enriched superparamagnetic grains no larger than several nanometers. According to the corresponding phase diagram [10], the Fe and Cr components form unlimited solutions at temperatures higher than the melting point (≈1600 K), while the supersaturated Fe_xCr_{1-x} (x = 50–70 at. %) solution possesses a higher Curie temperature (≈900 K). The necessity of

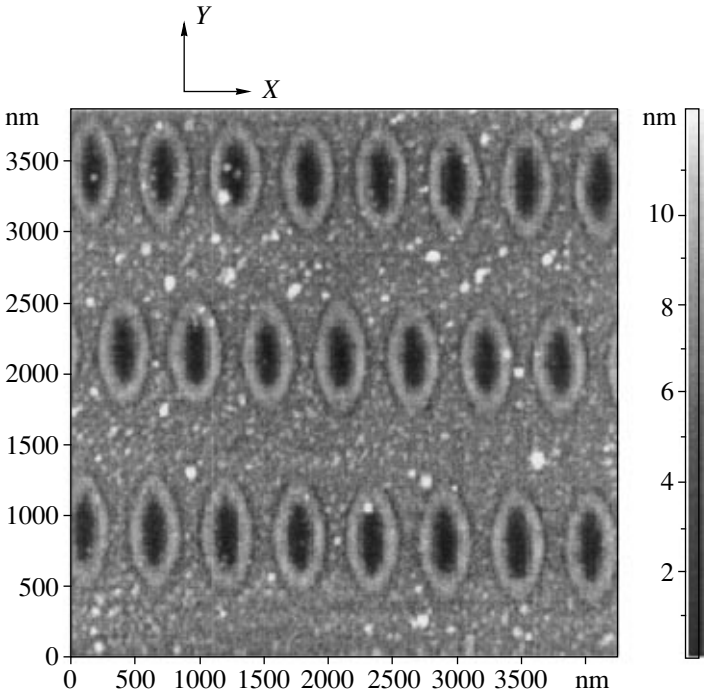

Fig. 3. Topography of the surface of a $Fe_{0.7}Cr_{0.3}$ layer after the irradiation with E = 300 mJ/cm^2. The AFM image.

achieving the liquid state upon laser heating in an attempt to accomplish magnetic transformation is corroborated by the fact that the melting and expelling of a liquid from the interference maxima (Fig. 3) are observed for a laser energy (300 mJ/cm^2) only slightly above the magnetic transformation threshold (220–240 mJ/cm^2). However, the most pronounced and well-interpreted magnetic structure is formed directly at the modification threshold (Figs. 1, 2), where the craters are as yet not formed at the surface.

It is not improbable that the observed increase in the "rectangularity" of the magnetization loops of the crater structures (Fig. 4) in the transverse direction can be explained by the interactions between the ferromagnetic regions (craters) via the superparamagnetic medium. This interaction becomes possible either because of the medium magnetization by the stray fields of the ferromagnetic regions or due to medium modification upon an increase in the cluster sizes and cluster approach. Evidently, the separation between craters and their aspect ratio decrease with increasing pulse energy. Since the distance between the elliptic craters along their minor axes is appreciably shorter than along the major axes (Fig. 3), the demagnetization effect in this direction is less pronounced. Thus, the direction of the easy magnetic axis in the resulting crater structures is likely determined by the competition of two factors: the interaction between the ferromagnetic regions via a magnetically soft (superparamagnetic) medium and a change in the shapes of these regions.

Note in conclusion that our experiments can be used to formulate the technological requirements on the variable parameters (concentration of the magnetic component, laser pulse energy and duration, angles of incidence, etc.) for producing gratings of magnetic single-domain elements with spacing in the far-submicron

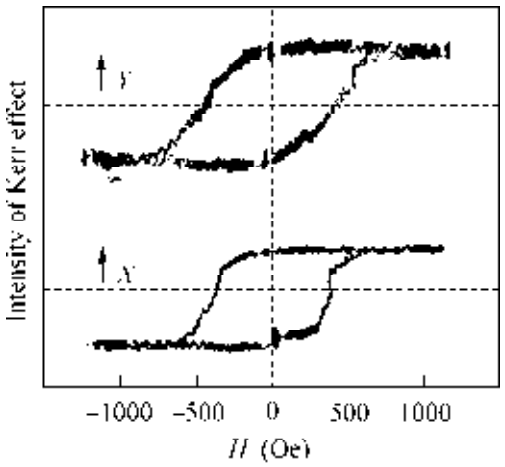

Fig. 4. Magnetization reversal curves for a $Fe_{0.7}Cr_{0.3}$ layer with the surface lattice of elliptically shaped craters (E = 300 mJ/cm^2). The loops are obtained for different orientations of H: along the major (Y) and minor (X) axes of ellipses.

range. The small sizes of the elements facilitate the realization of practically important physical properties (single-domain structure, rectangular hysteresis loops, short magnetization-reversal time, etc. [11]) for small magnetic objects.

This work was supported by the Russian Foundation for Basic Research, project no. 01-02-16445.

REFERENCES

1. C. Schwink, K. Emmerich, and U. Schulze, Z. Phys. B **31**, 385 (1978).
2. K. Takanashi, T. Sugawara, K. Hono, and H. Fujimori, J. Appl. Phys. **76**, 6790 (1994).
3. M. Ohkoshi, J. Appl. Phys. **63**, 2926 (1988).
4. K. Handrich and S. Kobe, *Amorphe Ferro- und Ferrimagnetika* (Akademie-Verlag, Berlin, 1980; Mir, Moscow, 1982).
5. N. I. Polushkin and N. N. Salashchenko, J. Magn. Magn. Mater. **124**, 347 (1993).
6. Yu. Blyakhman, N. I. Polushkin, A. D. Akhsakhalyan, *et al.*, Phys. Rev. B **52**, 10303 (1995).
7. S. Y. Chou, Proc. IEEE **85**, 652 (1997).
8. R. M. H. New, R. F. W. Pease, and R. L. White, J. Magn. Magn. Mater. **155**, 140 (1996).
9. J.-G. Zhu and H. N. Bertram, J. Appl. Phys. **66**, 1291 (1989).
10. O. Kubaschewski, *Iron-binary Phase Diagrams* (Springer-Verlag, Berlin, 1982; Metallurgiya, Moscow, 1985).
11. D. D. Awschalom and D. P. DiVincenzo, Phys. Today **48**, 43 (1995).

Translated by V. Sakun